

ACCEPTED MANUSCRIPT • OPEN ACCESS

## Minimizing Optical Measurement Time of Micro Spur Gears through Point Cloud Completion Techniques

To cite this article before publication: Ali Bilen *et al* 2025 *Meas. Sci. Technol.* in press <https://doi.org/10.1088/1361-6501/ae1d9c>

### Manuscript version: Accepted Manuscript

Accepted Manuscript is “the version of the article accepted for publication including all changes made as a result of the peer review process, and which may also include the addition to the article by IOP Publishing of a header, an article ID, a cover sheet and/or an ‘Accepted Manuscript’ watermark, but excluding any other editing, typesetting or other changes made by IOP Publishing and/or its licensors”

This Accepted Manuscript is © 2025 The Author(s). Published by IOP Publishing Ltd.



As the Version of Record of this article is going to be / has been published on a gold open access basis under a CC BY 4.0 licence, this Accepted Manuscript is available for reuse under a CC BY 4.0 licence immediately.

Everyone is permitted to use all or part of the original content in this article, provided that they adhere to all the terms of the licence <https://creativecommons.org/licenses/by/4.0>

Although reasonable endeavours have been taken to obtain all necessary permissions from third parties to include their copyrighted content within this article, their full citation and copyright line may not be present in this Accepted Manuscript version. Before using any content from this article, please refer to the Version of Record on IOPscience once published for full citation and copyright details, as permissions may be required. All third party content is fully copyright protected and is not published on a gold open access basis under a CC BY licence, unless that is specifically stated in the figure caption in the Version of Record.

View the [article online](#) for updates and enhancements.

# Minimizing Optical Measurement Time of Micro Spur Gears through Point Cloud Completion Techniques

Ali Bilen<sup>1\*</sup>, Max Decman<sup>1</sup>, Prof. Dr.-Ing. Florian Stamer<sup>2</sup>,  
Prof. Dr.-Ing. Gisela Lanza<sup>1</sup>

\*Corresponding Author

<sup>1</sup>Institute of Production Science, Karlsruhe Institute of Technology, Kaiserstraße 12, 76131 Karlsruhe, Germany

<sup>2</sup>Institute for Production Technology and Systems, Leuphana University Lüneburg, Universitätsallee 1, 21335 Lüneburg, Germany

E-mail: ali.bilen@kit.edu, max.dezman@partner.kit.edu

3rd of April 2025

## Abstract.

In micro gear manufacturing, quality assessment relies on full-geometry measurements to evaluate functional performance. Due to tolerances down to one micrometer, high-end metrology is essential. Optical systems enable fast, non-contact measurements and can, in principle, be used for full-gear scans. These scans serve as input for single-flank rolling simulations, which assess how geometric deviations affect functional behavior such as transmission accuracy. However, full scans remain time-consuming and often unsuitable for inline inspection due to the trade-off between speed and measurement uncertainty. We address this by proposing a partial-scan workflow, based on the observation that tool-induced deviations propagate periodically across gear teeth. This allows reconstruction of micrometer-accurate point clouds from a subset of teeth. We compare a deep learning-based completion network with an analytical reconstruction, evaluating both geometrically and functionally. While the deep learning approach shows higher geometric fidelity, it falls short in functional accuracy. This reveals a common gap in learning-based methods, where achieving geometric similarity may fail to preserve the underlying functional behavior. Our approach enables faster inspection while maintaining confidence in gear performance.

## 1 2 3 4 5 6 7 8 9 10 11 12 13 14 15 16 17 18 19 20 21 1. Introduction

22 Micro gears are key components in high-precision applications such as medical devices and microrobotics [1]. As miniaturization progresses, the demand for consistently manufactured, high-quality micro gears increases. Due to their small dimensions, even minor deviations in tooth flank geometry can severely affect functional performance, leading to vibration issues, transmission errors, or noise [2, 3, 4, 5]. Ensuring geometric and functional precision is therefore critical.

23 Unlike many other components, gears require a comprehensive quality assessment that goes beyond simple dimensional checks [1]. Detailed flank geometry must be captured and analyzed to assess characteristics such as noise, vibration, and harshness [4]. This can be achieved through tactile coordinate metrology, optical techniques like computed tomography or focus variation, or through functional testing methods such as single-flank rolling inspection [5, 2].

24 Although effective, both geometric and functional inspections are typically time-consuming [6]. Tight tolerances and high precision demands increase sensitivity to measurement uncertainty and limit throughput, especially in micro gear manufacturing. Recent studies have focused on accelerating optical workflows while maintaining accuracy [6]. Simulation-based functional assessments, such as single-flank rolling analysis using high-resolution point clouds, are promising alternatives [2], but still require full geometry acquisition.

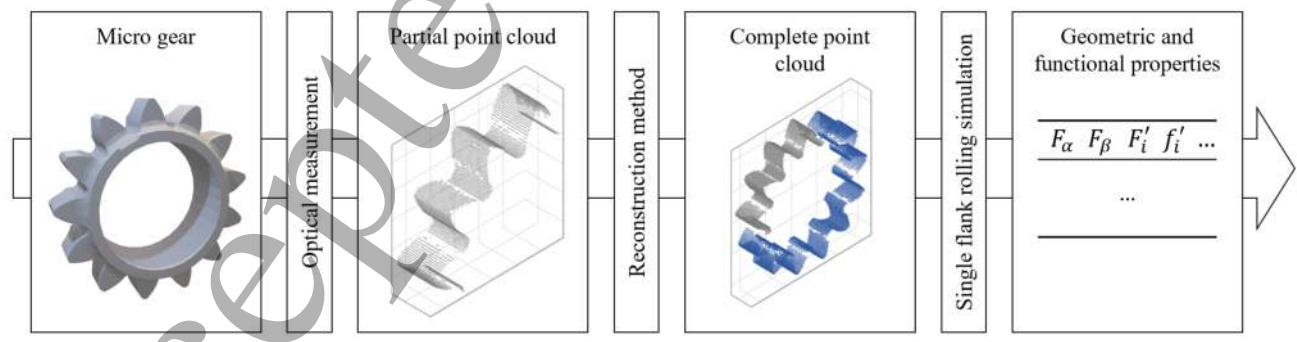
25 26 27 28 29 30 31 32 33 34 35 36 37 38 39 40 41 42 43 44 45 46 47 48 49 50 51 52 53 54 55 56 57 58 59 50 However, the highly regular structure of gears and the recurring nature of their deviation patterns offer great potential for point cloud completion. In this work, we explore whether full gear geometries

50 can be reconstructed from partial scans using only a small number of measured teeth, as illustrated in Figure 1. We investigate two approaches: one based on parametric gear geometry and another using deep neural networks trained to reconstruct full geometries from incomplete point cloud data. The network learns a latent representation of gear geometry, enabling it to infer missing surface regions from incomplete input data by leveraging patterns observed during training. Both approaches are evaluated through single-flank rolling simulations to assess their functional validity. Rather than demonstrating a complete inline system, this study provides a proof-of-method showing that partial optical measurements can be sufficient for accurate reconstruction and functional evaluation. These results highlight the potential of the approach as a step toward fast, reliable quality assessment and future inline inspection of micro gears.

51 52 53 54 55 56 57 58 59 60 In the following, we present the foundations of geometric and functional gear quality assessment. We then review developments in optical metrology, rolling simulation, and geometry reconstruction. Next, we describe our experimental setup, including gear measurement and point cloud generation. We then detail the reconstruction methods and evaluate their results functionally. Finally, we compare the approaches in terms of accuracy, robustness, and suitability for use in production environments.

## 2. Fundamentals

Micro gears demand stringent quality assessment through geometric and functional measurements to ensure reliable operation. In this section, we define the essential quality metrics that form the foundation



50 51 52 53 54 55 56 57 58 59 60 Figure 1: Conceptual schematic to improve measurement time.

of micro gear inspection. The general geometrical and functional quality characteristics of the gears are formalized in [7] and [8] which also specify the following measurement procedures.

### Geometric Quality Features

The geometric quality of micro gears is defined by four key deviations from the ideal involute: profile deviation  $F_\alpha$ , flank line deviation  $F_\beta$ , pitch deviation  $F_p$ , and runout deviation  $F_r$  [8, 9]. These parameters describe deviations in tooth form, alignment, spacing, and concentricity and serve as the basis for standardized gear quality evaluation.

Figure 2 illustrates the geometric deviations. The standardization of gear parameters as defined in [10] guarantees reproducibility at micrometer level accuracy, which is essential for high-precision applications in medical devices and robotic systems.

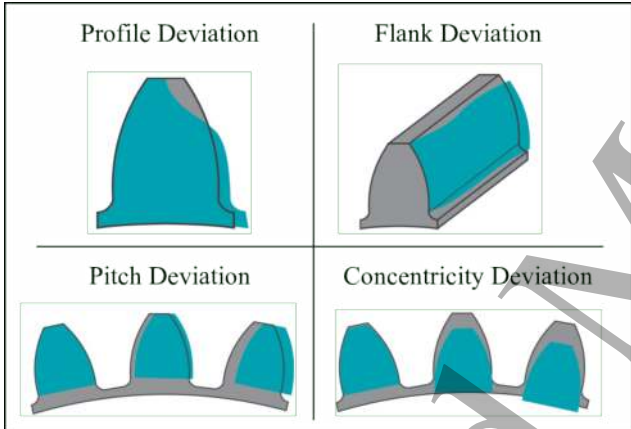


Figure 2: Geometric gear deviations, including profile, flank, pitch, and runout errors. Based on [11].

### Functional Quality Features

In this work, functional performance is evaluated using transmission error as the primary metric. Transmission error quantifies the deviation between the actual and ideal rotational displacement and is measured through single-flank and double-flank rolling tests [7]. In the single-flank test, the angular position of a test gear is recorded as it rolls against a master gear. The basic setup is illustrated in Figure 3, where transmission deviations emerge during meshing and are captured through angular measurement.

From these tests, the roll-in deviation  $f'_i$  which captures the maximum error within a single engagement, and the total transmission error  $F'_i$  which represents the peak deviation over a full revolution, are extracted. Additionally, the long-wave error  $f'_l$  and the short-wave error  $f'_k$  characterize low-frequency

shape deviations and high-frequency waviness, respectively [7]. These functional metrics reflect how geometric imperfections translate into torque irregularities under operating conditions [2].

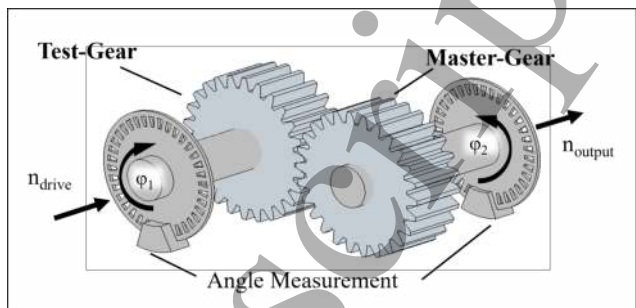


Figure 3: Setup of a single-flank rolling test, where the test gear rolls against a master gear. Angular deviations are recorded to determine the transmission error. Based on [5].

Figure 4 shows a typical transmission error curve obtained from the single-flank test. From this curve, key functional quality metrics such as runout error, jump error, and rolling deviation can be derived by analyzing the angular displacement trace.

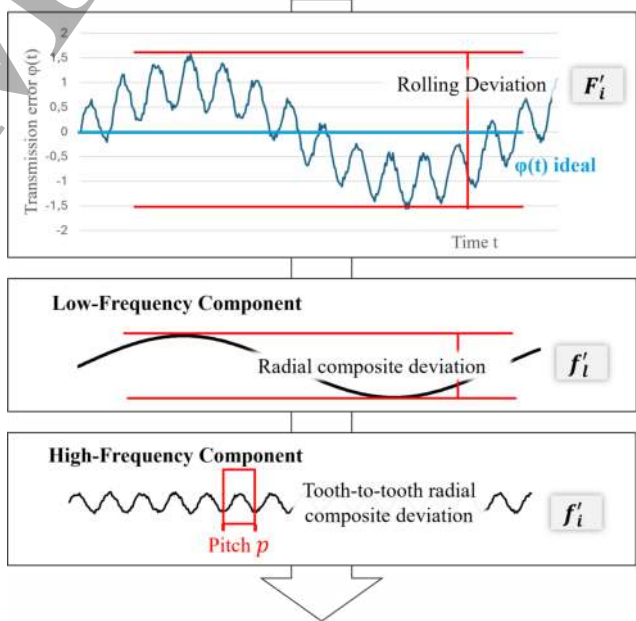


Figure 4: Evaluation of the transmission error curve from a rolling test. Functional deviations such as runout error, jump error, and rolling deviation are derived from the angular displacement trace. Based on [5].

### 1 2 3 4 5 6 7 8 9 10 11 12 13 14 15 16 17 18 19 3. State-of-the-art

1  
2  
3  
4  
5  
6  
7  
8  
9  
10  
11  
12  
13  
14  
15  
16  
17  
18  
19  
20  
21  
22  
23  
24  
25  
26  
27  
28  
29  
30  
31  
32  
33  
34  
35  
36  
37  
38  
39  
40  
41  
42  
43  
44  
45  
46  
47  
48  
49  
50  
51  
52  
53  
54  
55  
56  
57  
58  
59  
50  
51  
52  
53  
54  
55  
56  
57  
58  
59  
60 This chapter reviews the main techniques that enable modern micro gear inspection and reconstruction. First we examine focus variation as a fast, non-contact method for capturing gear surface geometry, chosen here for its favorable trade-off between acquisition time and resolution. We then consider single-flank rolling simulations as a direct measure of functional performance. We outline recent deep learning methods for reconstructing full geometries from sparse point clouds. Although each of these approaches has matured individually, no existing framework combines partial optical scans, completion methods and real-time functional simulation to enable inline quality assessment.

#### 19 20 21 22 23 24 25 26 27 28 29 30 31 32 33 34 35 36 37 38 39 40 3. Micro Gear Metrology

21  
22  
23  
24  
25  
26  
27  
28  
29  
30  
31  
32  
33  
34  
35  
36  
37  
38  
39  
40  
41  
42  
43  
44  
45  
46  
47  
48  
49  
50  
51  
52  
53  
54  
55  
56  
57  
58  
59  
60 The extensive literature review presented by Goch et al. [1], as an update to his foundational study from 2003 [12], represents one important contribution to the niche domain of micro gear metrology. Their analysis identifies the most relevant measurement technologies for capturing the geometry and functional characteristics of micro gears. Due to the miniature module sizes, typically below 0.3 mm, even slight deviations in geometry or surface finish can lead to significant functional impairments. Traditional tactile coordinate measuring techniques often reach their physical limits, as probe tip diameters are in the same order of magnitude as critical gear features, making reliable access to root and flank regions difficult [1, 13]. Computed tomography, while capable of capturing internal structures, suffers from long acquisition times and limited resolution for high aspect ratio geometries [1]. Optical methods have therefore gained increasing attention, as they offer non-contact access to steep surfaces and fine features with sub-micron resolution [1, 14]. In addition to capturing geometric parameters such as profile and helix deviations, surface-sensitive measurements are essential to assess wear and roughness that critically influence gear performance at the microscale [1, 15]. Overall, micro gear metrology requires a careful balance between resolution, measurement speed, and accessibility of complex geometries.

#### 50 51 52 53 54 55 56 57 58 59 60 Focus Variation for Geometric Quality Assessment

50  
51  
52  
53  
54  
55  
56  
57  
58  
59  
60 Focus variation is a non-contact optical technique that captures fine surface geometry by scanning an objective over a vertical range and computing a sharpness metric for each pixel [16]. This enables high-resolution 3D point clouds, even on steep and reflective surfaces. A typical setup is shown in Figure 5.

1  
2  
3  
4  
5  
6  
7  
8  
9  
10  
11  
12  
13  
14  
15  
16  
17  
18  
19  
20  
21  
22  
23  
24  
25  
26  
27  
28  
29  
30  
31  
32  
33  
34  
35  
36  
37  
38  
39  
40  
41  
42  
43  
44  
45  
46  
47  
48  
49  
50  
51  
52  
53  
54  
55  
56  
57  
58  
59  
60 Gauder et al. [14] demonstrated the successful inline integration of a Bruker Alicona  $\mu$ CMM for micro gear inspection. Their process achieved full 3D measurement with low uncertainty in under 3.5 minutes, well below the duration of tactile or CT methods. Critical regions such as steep root areas were captured through eccentric positioning, improving detectability at the cost of longer measurement time.

1  
2  
3  
4  
5  
6  
7  
8  
9  
10  
11  
12  
13  
14  
15  
16  
17  
18  
19  
20  
21  
22  
23  
24  
25  
26  
27  
28  
29  
30  
31  
32  
33  
34  
35  
36  
37  
38  
39  
40  
3. By optimizing vertical resolution and measurement width, the team showed that acceptable accuracy can be achieved within production cycle time. Ultimately, the method proved suitable for inline inspection. Remaining challenges include software stability and automation of cleaning and clamping.

1  
2  
3  
4  
5  
6  
7  
8  
9  
10  
11  
12  
13  
14  
15  
16  
17  
18  
19  
20  
21  
22  
23  
24  
25  
26  
27  
28  
29  
30  
31  
32  
33  
34  
35  
36  
37  
38  
39  
39  
40  
41  
42  
43  
44  
45  
46  
47  
48  
49  
50  
51  
52  
53  
54  
55  
56  
57  
58  
59  
60 Among available optical methods, focus variation offers the best balance of speed, resolution, and surface accessibility inline inspection. Confocal and interferometric techniques offer higher vertical resolution, but are limited by slower acquisition rates, while CT scanning entails longer measurement times and reduced surface fidelity [17].



1  
2  
3  
4  
5  
6  
7  
8  
9  
10  
11  
12  
13  
14  
15  
16  
17  
18  
19  
20  
21  
22  
23  
24  
25  
26  
27  
28  
29  
30  
31  
32  
33  
34  
35  
36  
37  
38  
39  
39  
40  
41  
42  
43  
44  
45  
46  
47  
48  
49  
50  
51  
52  
53  
54  
55  
56  
57  
58  
59  
60 Figure 5: Inline setup of the focus variation. Based on [18].

#### 50 51 52 53 54 55 56 57 58 59 60 Single Flank Rolling Simulations for Functional Assessment

1  
2  
3  
4  
5  
6  
7  
8  
9  
10  
11  
12  
13  
14  
15  
16  
17  
18  
19  
20  
21  
22  
23  
24  
25  
26  
27  
28  
29  
30  
31  
32  
33  
34  
35  
36  
37  
38  
39  
39  
40  
41  
42  
43  
44  
45  
46  
47  
48  
49  
50  
51  
52  
53  
54  
55  
56  
57  
58  
59  
60 Single-flank rolling simulations replicate the meshing of a test gear with a reference gear to quantify functional deviations such as transmission error [7]. Tools like Frenco Reany can generate rolling curves based on 3D STL data or 2D profile sections of the gear geometry, enabling virtual assessments of meshing quality without requiring physical contact.

1  
2  
3  
4  
5  
6  
7  
8  
9  
10  
11  
12  
13  
14  
15  
16  
17  
18  
19  
20  
21  
22  
23  
24  
25  
26  
27  
28  
29  
30  
31  
32  
33  
34  
35  
36  
37  
38  
39  
39  
40  
41  
42  
43  
44  
45  
46  
47  
48  
49  
50  
51  
52  
53  
54  
55  
56  
57  
58  
59  
60 Gauder et al. [3] employed such simulations to establish a functional quality control loop for the gear hobbing process. By linking simulated functional metrics to process parameters, quality feedback could be integrated into manufacturing. In a preceding study [2], the uncertainty of simulated single-flank test results was evaluated, showing that when properly calibrated simulations can offer reliable functional assessments within micrometre scale accuracy.

Point Cloud Completion with Deep Learning

Recent advances in deep learning have enabled the reconstruction of complete 3D geometries from sparse input data, with works such as PointNet [19] establishing a foundation by learning permutation-invariant features directly from raw point clouds. Several more advanced deep neural networks have since been proposed to address point cloud completion [20]. We outline the idea and architecture of the two models used for our approach and mention other promising models.

The Point Completion Network (PCN) [21] implements a two stage reconstruction scheme. First an encoder composed of convolutional layers and a global max pooling operation extracts a compact latent representation of the partial point cloud. Next a fully connected decoder produces a sparse global outline of the full geometry. To recover fine local detail PCN applies a learned deformation grid around each coarse point and predicts displacement vectors that densify and refine the surface. This coarse to fine process preserves overall form while capturing intricate flank features.

The Morphing and Sampling Network (MSN) [22] uses an iterative deformation approach. Its encoder employs multi-scale feature extraction to capture both global shape and local surface variation. Instead of generating an intermediate outline, MSN directly learns a continuous flow field that deforms the input cloud in successive steps. At each iteration, the network predicts displacement vectors that move existing points toward the missing regions. An adaptive sampling module then adds points in areas of high curvature and removes excess points where detail is sufficient. This dynamic sampling strategy yields high-fidelity reconstructions with efficient use of computational resources.

More recent transformer-based methods further boost reconstruction fidelity. SymmCompletion [23] enforces known symmetry during attention to improve global consistency and local detail. AdaPoinTr [24] builds integrates curvature-aware attention that adapts point weighting based on local surface complexity. These transformer models demonstrate rapid progress in point cloud completion but remain dependent on large high-quality training sets. Acquiring full three dimensional micro gear scans at micrometer resolution is time intensive and costly in itself. Consequently, extensive data augmentation is required to train networks that generalize to inline inspection scenarios.

While each of the reviewed techniques has matured independently, they are rarely used in combination. This highlights a clear opportunity to develop an inline system that combines rapid measurement, learned reconstruction and immediate

functional evaluation. To our knowledge no existing approach achieves this combination, leaving a critical gap in enabling inline quality control of micro gears.

## 4. Approach

This chapter details the dataset and workflow for evaluating partial-scan reconstruction methods in inline micro gear quality assessment. We begin with gear specifications and measurement acquisition, then describe preprocessing and augmentation steps, outline both reconstruction strategies, present training configurations, and finally explain the functional simulation setup.

### *Data Acquisition and Gear Specifications*

We utilize a dataset of 280 real, high-resolution point cloud scans of industrial micro gears manufactured with a module of 0.28 mm, a face width of 0.9 mm, a pitch diameter of 4.424 mm, and a root diameter of 3.22 mm. Each gear features 13 involute teeth. Scans were acquired using the focus variation microscope  $\mu$ CMM by Bruker Alicona. A measurement of the studied gear is illustrated in Figure 6. The measurement parameters were adapted from the optimized measurement program presented by Gauder et al. [14], which achieves a full-geometry scan time of approximately 3.48 minutes per gear. The specific acquisition settings, including magnification, tilt angle, and resolution, are listed in Table 1. This setup ensures high vertical and lateral resolution, but is not compatible with inline integration due to its long acquisition time.

While the optical scans provide sufficient fidelity for reconstruction and simulation, they differ in important aspects from the formal requirements of standardized gear inspection procedures such as ISO 1328 [25]. Focus variation produces irregular point clouds rather than measurements along predefined sampling traces, and perpendicular access to the gear surface replaces the tangential acquisition directions assumed in the standard. In addition, standardized references, evaluation paths, and uncertainty budgets prescribed in conventional accuracy grading are not established in our setup. Consequently, the scans are not intended for assigning ISO accuracy grades, but serve as a representative proof-of-method dataset for reconstruction and functional assessment studies.

In order to minimize rotational input variation on the rotation axis and guarantee consistency between samples, all gear measurements were aligned to a shared coordinate system and filtered to preserve only the relevant gear surface. The common rotational axis was defined by the clamping mandrel used during measurement. To extract the tooth regions we first

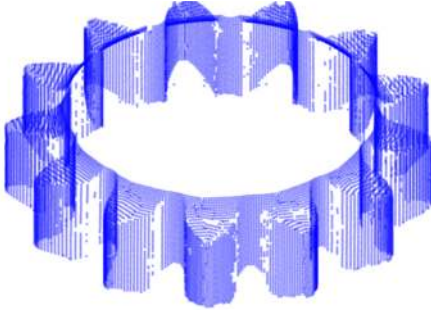


Figure 6: Full gear measurement.

Table 1: Optimized measurement parameters adapted from Gauder et al. [14].

Parameter	Value
Measurement strategy	Alicona Real3D
Magnification	800A (10x)
Tilt angle	+25°
Exposure time	1.810 ms
Contrast	0.6
Vertical resolution	0.030 µm
Lateral resolution	3.914 µm
Downsampling	16
Mean number of points	23,243
Width of measurement	1.312 mm
Polarization	Active
Precision mode	Off
Overlap percentage	19%
Outlier filter	0.93
<b>Mean measurement time</b>	<b>3.476 min</b>

identified the front surface of the point cloud using a histogram along the z-axis, which exhibits a distinct peak caused by the angled measurement process. Individual teeth were then detected by segmenting connected regions in the xy-plane. Figure 7 shows the extracted parts of the gear. For each partial input, only four consecutive adjacent teeth were retained, resulting in oriented partial point clouds with consistent spatial positioning across the dataset. Although we tested different tooth counts and alternative configurations, such as selecting every second tooth or sampling across the diameter, four consecutive teeth yielded the best reconstruction performance.

#### Data Augmentation

To increase dataset diversity and robustness, several augmentation strategies were applied to training and validation sets. These included mirroring each gear across a plane through the rotation axis and applying discrete rotational transformations corresponding to the number of gear teeth. For each rotation step, a different subset of teeth is presented as input, simulating various partial measurement scenarios.

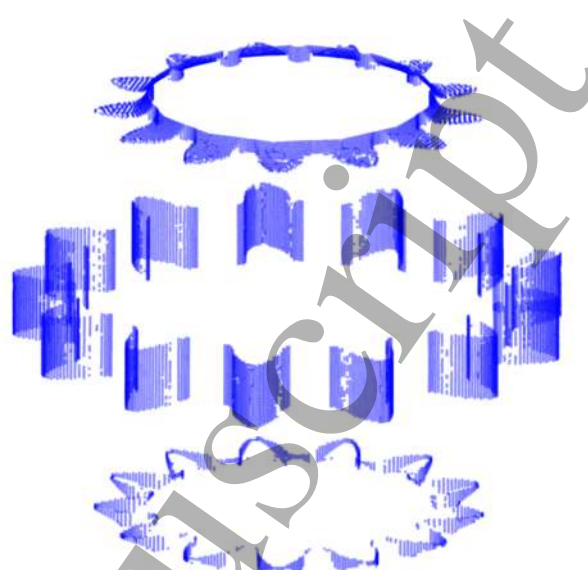


Figure 7: Gear decomposition for data processing.

These augmentation steps result in 26 unique samples per gear by combining mirroring with 13 discrete tooth-aligned rotations. The partial point clouds were randomly down-sampled to 2,048 points, while the full target geometries were represented with 8,192 points. These operations preserve the geometric structure of the gear while exposing the model to a broader range of unique spatial configurations.

Our dataset was divided into 70% training, 15% validation and 15% test sets. Only the training and validation sets were augmented, resulting in 5,096 and 1,092 point clouds, respectively. The test set remained non-augmented, allowing for a consistent and unbiased evaluation of model performance.

#### 4.1. Point cloud completion networks

In this work, we employ the point cloud completion networks PCN and MSN to reconstruct complete micro gear geometries from partial measurements. During training, we optimize the network parameters using either the Chamfer Distance (CD) or the Earth-Mover Distance (EMD) as the loss function. Let  $S_1$  and  $S_2$  denote two point clouds, where  $x \in S_1$  and  $y \in S_2$  represent individual points from each set. The Chamfer Distance provides an efficient measure of local similarity by averaging the squared Euclidean distances between each point in one set and its nearest neighbor in the other:

$$\begin{aligned} \mathcal{L}_{CD}(S_1, S_2) = & \frac{1}{|S_1|} \sum_{x \in S_1} \min_{y \in S_2} \|x - y\|_2 \\ & + \frac{1}{|S_2|} \sum_{y \in S_2} \min_{x \in S_1} \|x - y\|_2 \end{aligned} \quad (1)$$

In contrast, the Earth-Mover Distance evaluates the global similarity by determining the minimum cost required to transform one point cloud into the other:

$$\mathcal{L}_{EMD}(S_1, S_2) = \frac{1}{|S_1|} \min_{\phi: S_1 \rightarrow S_2} \sum_{x \in S_1} \|x - \phi(x)\|_2, \quad (2)$$

Although EMD generally offers a more faithful evaluation of overall similarity, its computational complexity is higher. To address this, we use an approximation method as implemented in [22].

Training was performed for 200 epochs with a batch size of 16, using either  $\mathcal{L}_{CD}$  or  $\mathcal{L}_{EMD}$  as the loss function. An initial learning rate of  $5e^{-3}$  was employed, decaying gradually to a minimum of  $1e^{-4}$ . The networks were optimized using the AdamW optimizer [26] with a weight decay of  $\lambda = 1e^{-4}$ . The training and validation loss curves of all models exhibited similar trends and stability, as shown in Figure 8. To mitigate overfitting, the model achieving the lowest validation loss during training was selected for evaluation.

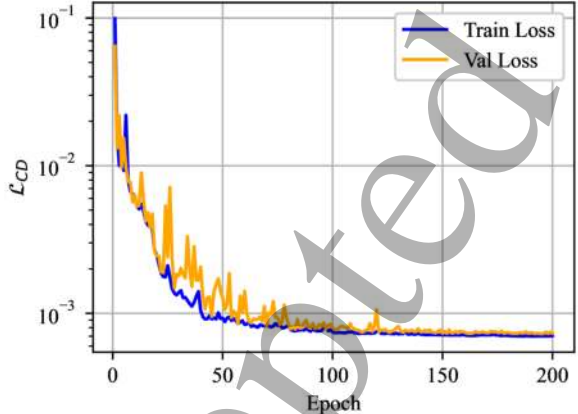


Figure 8: Train and validation loss curves for the MSN model using  $\mathcal{L}_{CD}$  for training.

#### 4.2. Geometric reconstruction

In addition to the methods presented, a geometric reconstruction (GA) baseline model is implemented for comparison. This approach reconstructs the gear geometry by iteratively duplicating existing teeth and placing them into unmeasured gaps based on their

relative positions. The reconstruction begins by inserting the first available measured tooth segment into the nearest missing position in clockwise direction and continuing with the next available segment until all gaps are filled. This method exploits the rotational symmetry of the gear and assumes structural consistency between neighboring teeth. The resulting point cloud is resized to 8,192 points either by random sampling or interpolation by choosing a random point and adding a point halfway to its closest neighbor.

#### 4.3. Functional simulation

Reconstructed and ground-truth clouds are evaluated with single-flank rolling simulations in Frenc Reany. The simulation outputs directly quantify transmission error under load and reveal how geometric reconstruction errors impact functional performance.

This comprehensive setup enables direct comparison of geometric fidelity and functional reliability for inline micro gear quality control. The reconstruction models can be trained on new gear designs to accommodate different modules and tooth counts. Each partial scan is processed with minimal latency, enabling real-time inline integration.

### 5. Point cloud reconstruction

The trained models are evaluated using the reserved test data with the different distance measures to the ground truth (GT). The results are summarized in Table 2.

Table 2: Model inference quality comparison using the test data set. Models highlighted with <sup>1</sup> and <sup>2</sup> are trained using  $\mathcal{L}_{CD}$  and  $\mathcal{L}_{EMD}$  respectively.

	GA	PCN <sup>1</sup>	PCN <sup>2</sup>	MSN <sup>1</sup>	MSN <sup>2</sup>
$\mathcal{L}_{CD}[10^4] \downarrow$	1.74	2.29	1.44	1.96	1.76
$\mathcal{L}_{EMD}[10^3] \downarrow$	12.87	14.24	10.82	19.33	12.61

The distance measures to the GT of all models including the GA have similar orders of magnitude. The models trained on  $\mathcal{L}_{EMD}$  have a consistently better score when comparing it to their trained models with  $\mathcal{L}_{CD}$ .

A sample of predictions were displayed for further analysis. The simulation software requires a uniformly distributed point cloud for the evaluation. If no structural features of the tooth surfaces are recognizable, the simulation cannot be carried out. A subset of predictions are illustrated in Figure 9 where the coloring highlights the distance of the measured point to the master geometry. The master geometry is used as a reference because the goal is not to

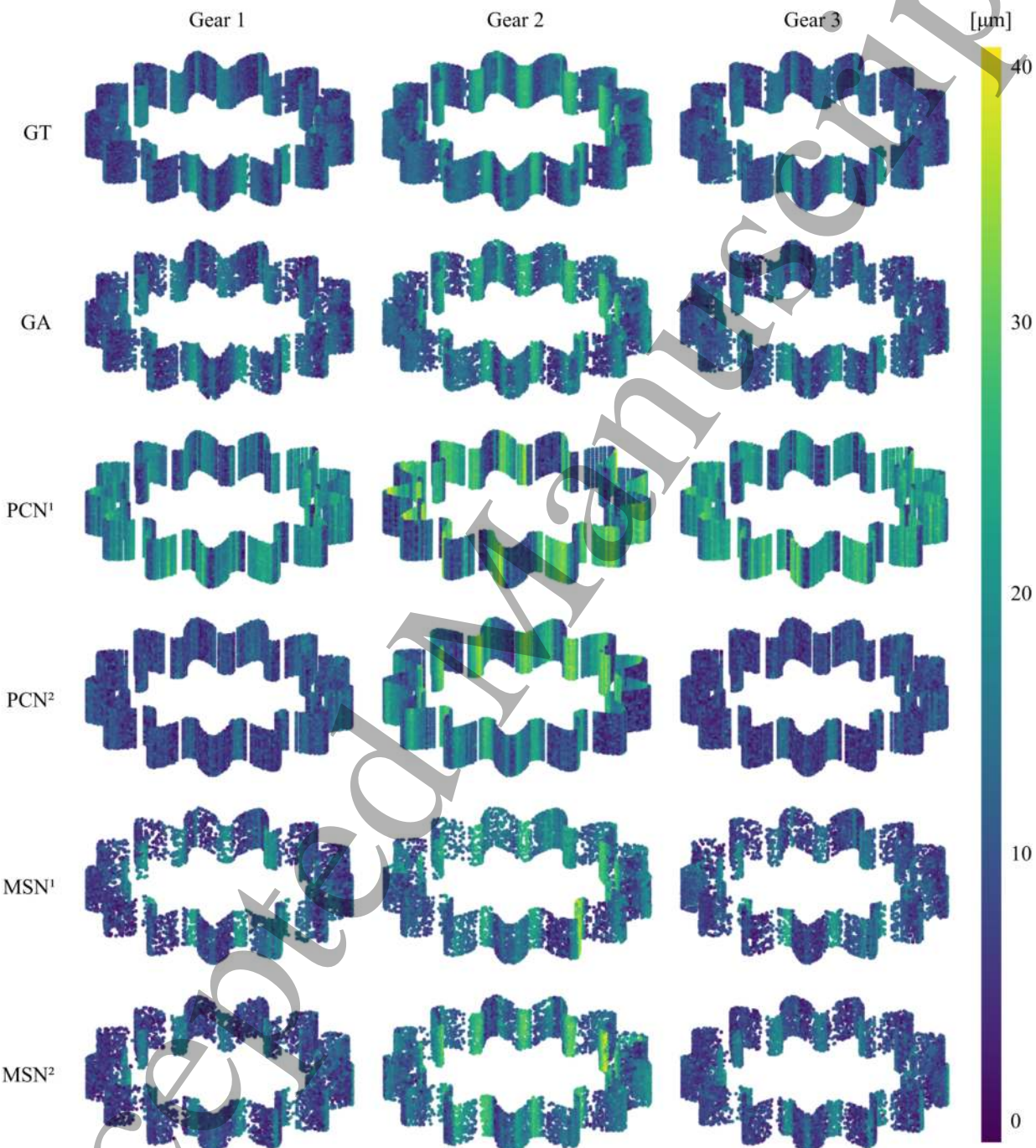


Figure 9: Distances to the master geometry from predictions in  $\mu\text{m}$ .

match individual points exactly, but to capture the correct shape. Accordingly, the color gradients should exhibit similar patterns if the overall geometry is preserved. The predictions of all models show the shape of our desired micro gear. However, the distances to the real geometry deviate between models. The colored representation shows that the models trained with  $\mathcal{L}_{EMD}$  has a good agreement of the tooth flank deviations to the real point clouds. This is particularly noticeable for the MSN model, where the tooth gaps show a deviation similar to that in the real point cloud. In contrast, the models trained with  $\mathcal{L}_{CD}$  show stronger deviations along the teeth that do not correspond to reality.

A positive aspect about the PCN models is the regular spacing of the predicted points. The MSN models show a direct difference. The micro gear structure is recognizable, but the point distributions of the model show a non-uniformity compared to the PCN architecture. The point distribution of the prediction is more consistent with the original input, which was reduced by random sampling. The structure of the input can be inferred from the GA in Figure 10, as this copies the existing input.

This behavior can further be seen the two-dimensional visualization in Figure 10 where the gear is *unrolled*. It uses the same coloring scheme as the three-dimensional visualization. It further highlights the nearly identical deviation from the GT to the GA with the other models performing worse.

## 6. Simulation result

For each GT and predicted point cloud, the simulation software computes the geometric and functional properties of the left and right tooth flanks based on the gear characteristics outlined in Section 2. The result is averaged across both tooth flanks. Figure 11 shows the boxplots of the simulation results.

The key takeaway from the boxplots is the good performance of the geometric approach. For all of the six selected parameters it only has very slight deviation from the GT. Similar behavior is achieved by the PCN<sup>2</sup> model for  $F'_i$  and  $f'_k$ . Generally speaking, the MSN models show less accordance to the GT. For easier comparisons, the median of the feature values is noted in Table 3 and the median difference to the GT is noted in Table 4.

The results are interpreted using Table 4. The simulation shows that the models trained with  $\mathcal{L}_{EMD}$  perform better than its counterpart except for the features  $F_\alpha$  and  $F_\beta$ . The values of the predictions fall in the range of measurement uncertainty described in [2] for specific features. The geometric model shows the highest accordance to the ground truth overall.

Table 3: Feature simulation results for each model.

Feature	GT	GA	PCN <sup>1</sup>	PCN <sup>2</sup>	MSN <sup>1</sup>	MSN <sup>2</sup>
$F_\alpha$	10.33	10.31	10.99	8.85	8.22	7.17
$F_\beta$	1.18	1.31	1.04	0.71	2.08	3.59
$F_p$	5.90	5.82	13.04	11.27	16.47	10.08
$F'_i$	16.78	16.81	25.30	18.95	34.18	31.58
$f'_l$	4.74	4.62	7.88	6.97	8.86	4.71
$f'_k$	13.14	13.05	25.35	13.77	31.96	30.54

Table 4: Median simulation differences to GT across gear quality features.

Feature	GR	PCN <sup>1</sup>	PCN <sup>2</sup>	MSN <sup>1</sup>	MSN <sup>2</sup>
$F_\alpha$	-0.04	0.80	-1.42	-1.77	-3.01
$F_\beta$	0.14	-0.15	-0.46	0.90	2.39
$F_p$	0.03	6.97	4.94	10.08	3.66
$F'_i$	0.10	10.39	2.09	16.33	12.19
$f'_l$	0.04	2.95	2.75	4.33	0.40
$f'_k$	-0.02	12.41	0.70	18.43	12.98

## 7. Discussion and conclusions

The tests show that the base belief model with the geometric approach for reconstructing point clouds has a greater predictive power with regard to the quality characteristics compared to the learning based architectures. Despite a larger deviation from the original point cloud using the distance metrics, the model delivers better results in the single-flank rolling simulation. These features are of crucial importance for practical use in the evaluation of micro gears. While the proposed approach reduces measurement time, our experiments confirm that deviations in the reconstructed quality features remain and must be explicitly considered. Further improvements could be achieved by fine-tuning the loss functions to incorporate topological information, as the current metrics evaluate only point-wise accuracy and not overall shape fidelity.

The ability to retrain both neural models on new gear variants ensures adaptability to different modules tooth counts and design features. Moreover, the near-instant processing of partial scans demonstrates the feasibility of real-time analysis in principle, supporting prospects for deployment in quality control workflows. These factors demonstrate the feasibility of automated high-throughput inspections in production environments.

In conclusion, the analytical method provides a dependable foundation for inline micro gear quality control. Optimized learning-based approaches hold promise for scalable automated inspection once they incorporate domain-specific knowledge and expanded training data. Together with explicit consideration

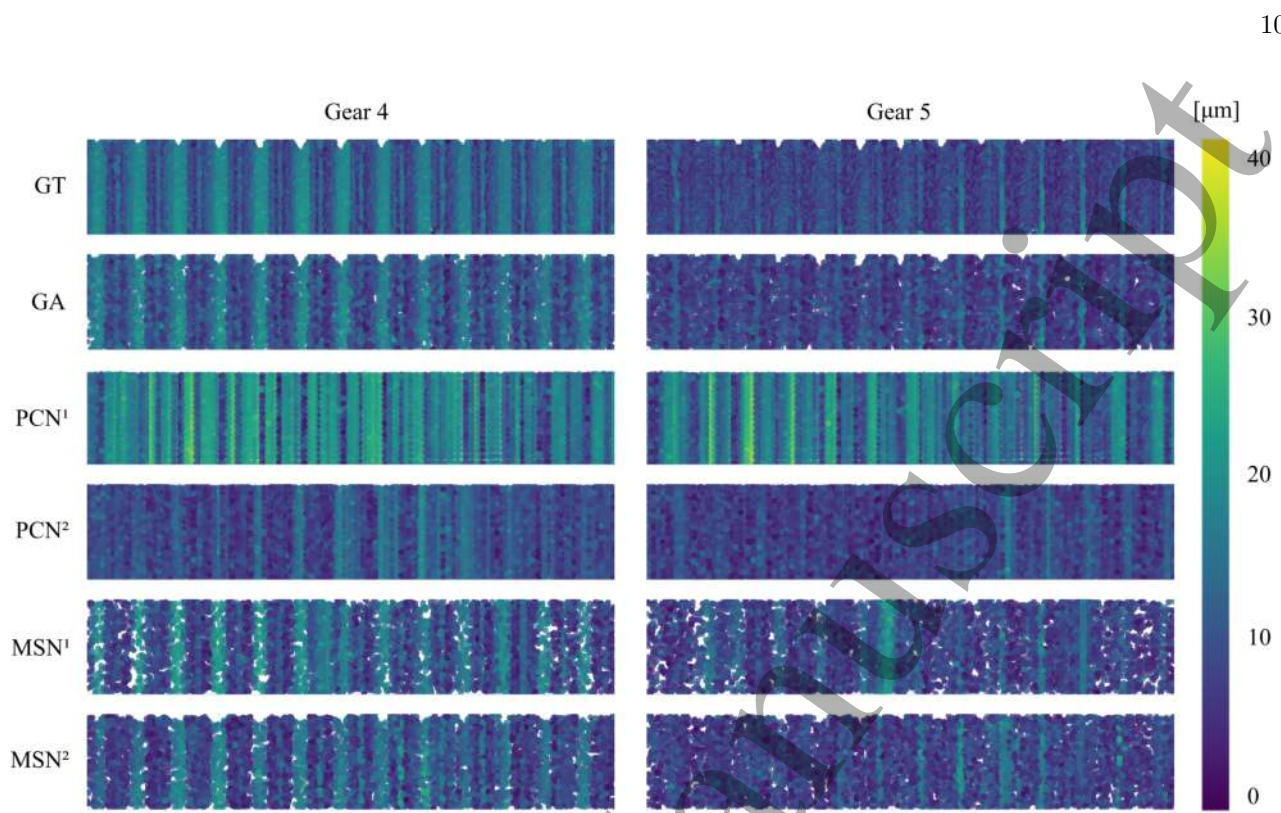


Figure 10: Distances to the master geometry in  $\mu\text{m}$  in a flat view.

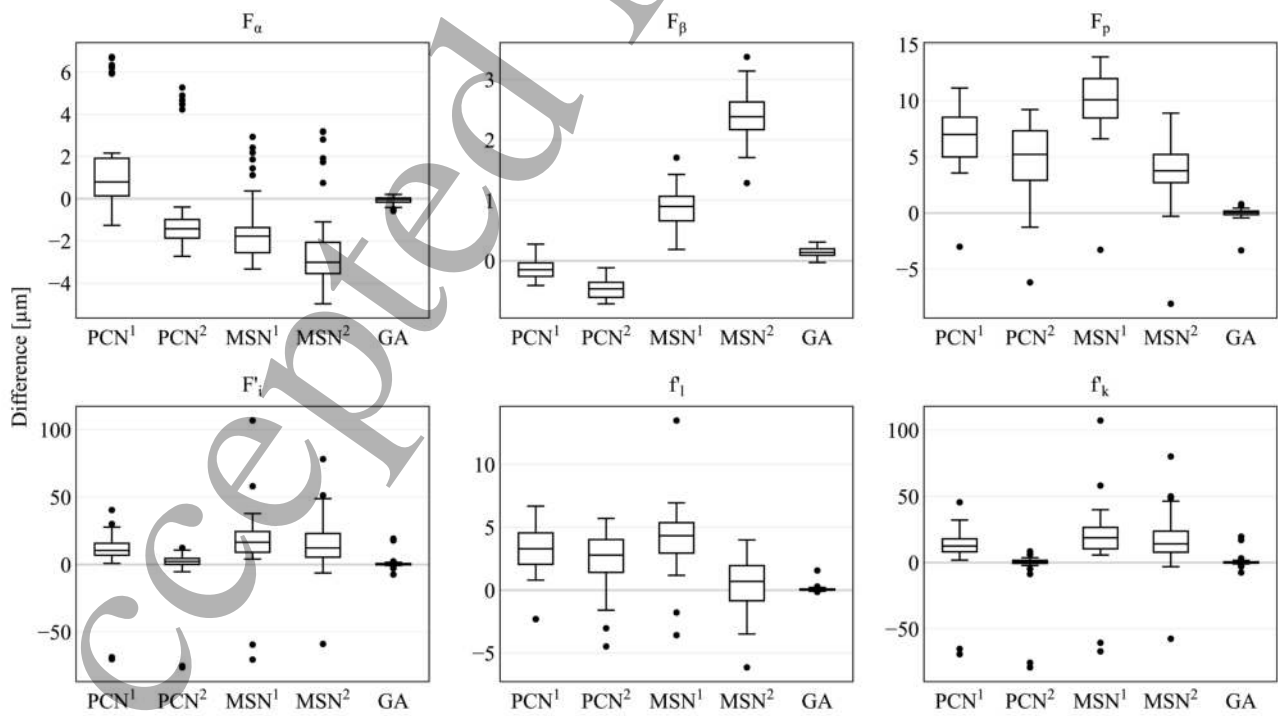


Figure 11: Boxplot of the simulation results for each gear with cutoff at  $3\sigma$ .

1  
2  
3  
4  
5  
6  
7  
8  
9  
10  
11  
12  
13  
14  
15  
16  
17  
18  
19  
20  
21  
22  
23  
24  
25  
26  
27  
28  
29  
30  
31  
32  
33  
34  
35  
36  
37  
38  
39  
40  
41  
42  
43  
44  
45  
46  
47  
48  
49  
50  
51  
52  
53  
54  
55  
56  
57  
58  
59  
60  
of measurement and reconstruction deviations, these strategies pave the way toward future inline evaluation of micro gears in advanced manufacturing workflows.

## Data availability

Due to legal constraints, the data cannot be shared publicly. The data supporting this study's findings can be obtained from the authors upon reasonable request.

## Acknowledgments

This paper was developed as part of the research and development project *INSPIRE: Intelligent Hybrid Decision Support Based on Multimodal AI for Product Development*. The project is funded by the German Research Foundation (project number 543072266) within the Priority Program *Hybrid Decision Support in Product Development*. The authors thank the German Research Foundation for its support.

## References

- [1] Goch G, Guenther A, Peng Y and Ni K 2023 *CIRP Annals* **72** 725–751 ISSN 0007-8506
- [2] Gauder D, Bott A, Gölz J and Lanza G 2023 *Computers in Industry* **146**
- [3] Gauder D, Gölz J, Jung N and Lanza G 2023 *Computers in Industry* **144** 103799
- [4] Neubauer P 2019 *Konzeption und Auslegung von geräuschoptimierten inäquidistanten Verzahnungen* Berichte aus der Akustik (Düren: Shaker Verlag) ISBN 9783844070965
- [5] Klocke F and Brecher C 2017 *Zahnrad- und Getriebetechnik: Auslegung – Herstellung – Untersuchung – Simulation* Hanser eLibrary (Carl Hanser Verlag) ISBN 9783446431409
- [6] Gauder D, Gölz J, Biehler M, Diener M and Lanza G 2021 *CIRP Journal of Manufacturing Science and Technology* **35** 209–216 ISSN 17555817
- [7] 2608 V R 2001 Einfanken- und zweifanken-wälzprüfung an zylinderrädern, kegelrädern, schnecken und schneckenrädern
- [8] 1 V R B 2024 Messen und prüfen von verzahnungen. auswertung von profil- und flankenlinienmessungen
- [9] 3960 D 1987 Bezugsprofile für evolventenverzahnungen an stirnrädern (zylinderrädern) – begriffe, anordnung der bezugsprofile
- [10] 21771-1 I 2024 Cylindrical involute gears and gear pairs — part 1: Concepts and geometry
- [11] WENZEL Precision GmbH 2025 Gearing: Quality Characteristics and Tooth Flank Modifications [https://www.metromec.ch/images/pdf/WENZEL\\_Poster\\_Verzahnungsparameter.pdf](https://www.metromec.ch/images/pdf/WENZEL_Poster_Verzahnungsparameter.pdf) poster, accessed on May 29, 2025
- [12] Goch G 2003 *CIRP Annals* **52** 659–695 ISSN 0007-8506
- [13] Härtig F, Schwenke H and Weiskirch C 2002 Messung von mikroverzahnungen *VDI Berichte* vol 1673 pp 247–258
- [14] Gauder D, Gölz J, Bott A, Jung N and Lanza G 2022 *tm - Technisches Messen* **89** 594–611
- [15] Härtig F, Kniel K and Rost K 2009 Messung von mikroverzahnung Tech. Rep. 5671(908) FVA-Forschungsvorhaben
- [16] Schuth M and Buerakov W 2017 *Handbuch Optische Messtechnik* (Carl Hanser Verlag) ISBN 9783446436619
- [17] Gauder D, Gölz J, Bott A, Stein M and Lanza G 2024 *Measurement Science and Technology* **35** 105013
- [18] Bruker Alicona 2025 Optisches Koordinatenmessgerät zur vollflächigen 3D-Messung <https://www.alicona.com/de/produkte/optisches-koordinatenmessgeraet> webpage, accessed on May 29, 2025
- [19] Charles R Q, Su H, Kaichun M and Guibas L J 2017 Pointnet: Deep learning on point sets for 3d classification and segmentation *2017 IEEE Conference on Computer Vision and Pattern Recognition (CVPR)* pp 77–85
- [20] Fei B, Yang W, Chen W, Li Z, Li Y, Ma T, Hu X and Ma L 2022 *IEEE Transactions on Intelligent Transportation Systems* **23** 22862–22883
- [21] Yuan W, Khot T, Held D, Mertz C and Hebert M 2018 Pcn: Point completion network *2018 International Conference on 3D Vision (3DV)* pp 728–737
- [22] Liu M, Sheng L, Yang S, Shao J and Hu S M 2020 *Proceedings of the AAAI Conference on Artificial Intelligence* **34** 11596–11603
- [23] Yan H, Li Z, Luo K, Lu L and Tan P 2025 *Proceedings of the AAAI Conference on Artificial Intelligence* **39** 9094–9102
- [24] Yu X, Rao Y, Wang Z, Lu J and Zhou J 2023 *IEEE Transactions on Pattern Analysis and Machine Intelligence* **45** 14114–14130
- [25] 1328-1 I 2013 Cylindrical gears – iso system of accuracy – part 1: Definitions and allowable values of deviations relevant to corresponding flanks of gear teeth
- [26] Loshchilov I and Hutter F 2019 Decoupled weight decay regularization (*Preprint* 1711.05101) URL <https://arxiv.org/abs/1711.05101>